

The Isophotic Metric and Its Application to Feature Sensitive Morphology on Surfaces

Helmut Pottmann¹, Tibor Steiner¹, Michael Hofer¹, Christoph Haider², and Allan Hanbury³

¹ Geometric Modeling and Industrial Geometry Group, Vienna Univ. of Technology
Wiedner Hauptstrasse 8-10. A-1040 Wien, Austria
{pottmann,tibor,hofer}@geometrie.tuwien.ac.at,

<http://www.geometrie.tuwien.ac.at>

² Advanced Computer Vision, Tech Gate Vienna
Donau-City-Strasse 1. A-1220 Wien, Austria

haider@acv.ac.at, <http://www.acv.ac.at>

³ Pattern Recognition and Image Processing Group, Vienna Univ. of Technology
Favoritenstrasse 9/1832. A-1040 Wien, Austria

hanbury@prip.tuwien.ac.at, <http://www.prip.tuwien.ac.at>

Abstract. We introduce the isophotic metric, a new metric on surfaces, in which the length of a surface curve is not just dependent on the curve itself, but also on the variation of the surface normals along it. A weak variation of the normals brings the isophotic length of a curve close to its Euclidean length, whereas a strong normal variation increases the isophotic length. We actually have a whole family of metrics, with a parameter that controls the amount by which the normals influence the metric. We are interested here in surfaces with features such as smoothed edges, which are characterized by a significant deviation of the two principal curvatures. The isophotic metric is sensitive to those features: paths along features are close to geodesics in the isophotic metric, paths across features have high isophotic length. This shape effect makes the isophotic metric useful for a number of applications. We address feature sensitive image processing with mathematical morphology on surfaces, feature sensitive geometric design on surfaces, and feature sensitive local neighborhood definition and region growing as an aid in the segmentation process for reverse engineering of geometric objects.

1 Introduction

The original motivation for the present investigation comes from the automatic reconstruction of CAD models from measurement data of geometric objects. In this area, called *reverse engineering of geometric objects*, a variety of shape classification methods have been developed, which aim at a segmentation of the measurement data into regions of the same surface type [26]. Particularly for traditional geometric objects, where most of the surfaces on the boundary of the object are fundamental shapes, the surfaces are often separated by edges

or smoothed edges, so-called blending surfaces. Thus, it is natural to look at geometric processing tools on surfaces which are sensitive to such features.

Inspired by image processing, which frequently uses *mathematical morphology* for basic topological and geometric operations [9,22], we have been looking for similar operations on surfaces. However, we found that just a few contributions [10,13,17,19,20,28] extend morphology to curved manifolds or meshes and cell decompositions on curved manifolds; none of these papers deals with the behavior at features. Thus, we will focus here on *feature sensitive mathematical morphology on surfaces*. We implement this through the use of adaptive structuring elements (SE), which change their shape and/or size based on either spatial position [2] or image content. The latter has been used, for example, in range image processing [27]. In these images, the pixel values represent distances to the detector, and hence they can be used to adapt the SE size to the expected feature size. To define appropriate SEs, we have developed an adapted metric on a surface, which we call *isophotic metric*. In this metric, the length of a surface curve depends not only on the curve, but also on the surface normal field along it. SEs, which are geodesic discs in the isophotic metric, behave in the right way at features that are characterized by a significant deviation of the two principal curvatures.

The isophotic metric also simplifies the definition of local neighborhoods for shape detection, the implementation of region growing algorithms and the processing of the responses from local shape detection filters (images on surfaces). For example, the neighborhoods of a point shown in Fig. 2 are not equally useful for local shape detection: The neighborhood based on the Euclidean metric (left) flows across the feature. However, the other neighborhoods (middle and right) respect the feature and are more likely to belong to the same surface type in an engineering object. Another example is depicted in Fig. 6: Region growing based on a feature sensitive metric can easily be stopped at features. Yet another application is design on surfaces: geodesics in a feature sensitive metric nicely follow features (Fig. 3) and morphology in such a metric could be used for artistic effects which are in accordance with the geometry of the surface (Fig. 7).

1.1 Previous Work

Mathematical morphology provides a rich and beautiful mathematical theory as well as a frequently used toolbox for basic topological and geometric operations on images [9,22]. Almost all of the work in discrete morphology is in \mathbb{R}^n , where the group of translations generates in a natural way the geometry of Minkowski sums. The latter are the basic building block for further powerful morphological operations. A few contributions go beyond this framework and in a direction which is close to our approach. As long as we are looking just for topological neighborhoods in meshes as discretizations of curved surfaces, we may use morphology on graphs [10,28]. The special case of 2D triangle meshes with the Delaunay property has been investigated by Lomenie et al. [13]. Topological neighborhoods on triangle meshes are also employed in a paper by Rössl et al. [20], which uses morphology for the extraction of feature lines on surfaces.

A basic problem in the extension of morphology to surfaces is the fact that there are no really useful translations, since parallel transport known in differential geometry is path dependent in case of non-vanishing Gaussian curvature. This problem has been addressed [19], but to our knowledge the studies have not been pursued towards efficient algorithms and practical applications. A simple geometric way to overcome the lack of translations is the use of approximants to *geodesic circles* as local neighborhoods (positions of the structuring element). The continuous viewpoint leads to morphology based on the distance function. There is beautiful work on this topic, mainly based on mathematical formulations with partial differential equations (PDE); see [1,4,21] and the references therein. The present paper is also related to geodesic active contours [3,21] in the sense that an appropriate Riemannian metric simplifies the formulation of the problem.

1.2 Contributions of This Paper

In our work we also use the PDE formulation; however, the metric and the resulting distance functions are more general. The distance functions we derive are based on the Gaussian mapping γ from a surface Φ to the unit sphere S^2 , a basic concept in differential geometry [6]. The main contributions of our work are the following:

- We define the isophotic metric, study its basic geometric properties, and discuss its analytical treatment for relevant surface representations (Sect. 2).
- The governing equations of distance fields in the new metric are elaborated and efficiently solved in a numerical way (Sect. 3).
- We introduce feature sensitive morphology on surfaces, which is based on the new metric and present applications in Computer Aided Design (Sect. 4).

2 The Isophotic Metric

Let us consider a surface $\Phi \subset \mathbb{R}^3$. We assume that we have chosen, at least locally, a continuous orientation of the unit normal vectors of Φ ; $\mathbf{n}(\mathbf{p})$ denotes the unit normal vector at the point $\mathbf{p} \in \Phi$. The *Gaussian map* $\gamma : \Phi \rightarrow S^2$ from Φ to the unit sphere S^2 maps a surface point \mathbf{p} to the point $\mathbf{n}(\mathbf{p}) \in S^2$ (see e.g. [6]). The preimage γ^{-1} of a circle $c \subset S^2$ is a curve on Φ , called an *isophote*. The surface normals along an isophote form a constant angle with the rotational axis of c . These curves of equal brightness in a very simple illumination model have been studied in classical constructive geometry; more recently they have been used in Computer Aided Design for quality inspection of surfaces [16]. We now define the *purely isophotic metric* on a surface as follows: *The isophotic length of a curve c on the surface is the Euclidean length of its Gaussian image curve $\gamma(c) \subset S^2$.* This metric obviously has the following simple properties:

- The shortest distance between two surface points is the angle ($\in [0, \pi]$) between their surface normals.

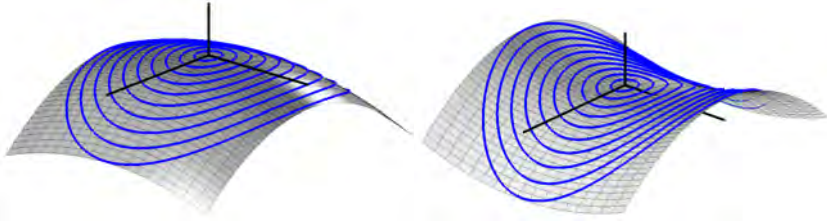


Fig. 1. Isophotes on an elliptic paraboloid (left) and a hyperbolic paraboloid (right).

- Let us fix a point $\mathbf{m} \in \Phi$. A *geodesic circle* in the isophotic metric, i.e. the set of all points $\mathbf{p} \in \Phi$ that lie at constant isophotic distance r to \mathbf{m} , is an *isophote* c_r . The Gaussian image of this isophote is a circle with center $\gamma(\mathbf{m})$ and spherical radius r .
- A *geodesic* g on Φ in the sense of the isophotic metric possesses as Gaussian image a geodesic on the unit sphere, i.e. a great circle. Let a_g denote the rotational axis of this circle. Then, at each point \mathbf{p} of g the surface normal $\mathbf{n}(\mathbf{g})$ is orthogonal to a_g . Considering a parallel projection in direction of a_g , the curve g is a *silhouette (contour generator)* on Φ . These curves have been extensively studied in constructive geometry and in Computer Vision (see e.g. [5]).

Example 1: Consider the paraboloid

$$\Gamma : 2z = \kappa_1 x^2 + \kappa_2 y^2. \tag{1}$$

Let us compute the isophotic geodesic circles with center at the origin, i.e., the isophotes for the direction $\mathbf{e} = (0, 0, 1)$. The direction of the normal at a surface point is given by the vector $(\kappa_1 x, \kappa_2 y, -1)$. The angle α between the normal $\mathbf{n}(\mathbf{p})$ at an arbitrary point $\mathbf{p} \in \Gamma$ and \mathbf{e} satisfies $\cos^2 \alpha = 1/(\kappa_1^2 x^2 + \kappa_2^2 y^2 + 1)$. Thus, the isophotes to $\cos^2 \alpha = c^2 = \text{const}$ are given by

$$\kappa_1^2 x^2 + \kappa_2^2 y^2 = K^2, \quad \text{with} \quad K^2 := \frac{1}{c^2} - 1. \tag{2}$$

In the xy -plane, these curves are concentric and similar ellipses. In \mathbb{R}^3 , (2) describes elliptic cylinders which intersect the paraboloid Γ in the actual isophotes (see Fig. 1). Note that the ratio of axis lengths of the ellipses (2) is $\rho_1 : \rho_2$, where $\rho_i := 1/|\kappa_i|$ are the principal curvature radii of Γ at the origin. We have used this example since it reveals important information for the general case as well. We may approximate any regular C^2 surface Φ at an arbitrary point \mathbf{m} up to second order by a paraboloid $\Gamma(\mathbf{m})$. In a local Cartesian frame with origin at \mathbf{m} and with the principal curvature directions and the surface normal as coordinate axis directions this paraboloid is written in the form (1). Here, κ_i are the principal curvatures of Φ and Γ at \mathbf{m} . Our example now describes the behavior of ‘small’ isophotes around \mathbf{m} . Viewing the family of shrinking isophotes for $K \rightarrow 0$ as a curve evolution (cf. Fig. 1), we may say in usual terminology, that

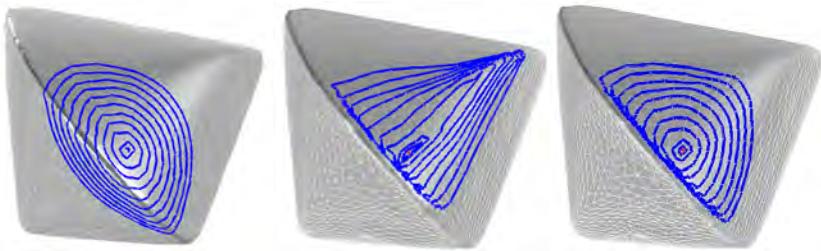


Fig. 2. Approximate geodesic circles on a triangle mesh in the Euclidean metric (left), purely isophotic metric (middle) and isophotic metric (right).

this family shrinks to an elliptic point with axis ratio $\rho_1 : \rho_2$. If we magnify the isophotes during the evolution so that they keep e.g. their length, the limit is an ellipse in the tangent plane at \mathbf{m} , whose axes agree with the principal axes of the surface Φ and whose axis ratio is $\rho_1 : \rho_2$. The discussion of this example shows the following two important facts, the first of which is desirable but the second one is not:

- Isophotic geodesic discs around a center \mathbf{m} are interesting candidates for structuring elements in mathematical morphology on surfaces. They are elongated in direction of large normal curvature radii and they are of smaller width in direction of small normal curvature radii. This anisotropic behavior is useful if we are working along surface features which are characterized by a significant deviation between the two principal curvatures, e.g. along smoothed edges, blends and similar curve-like features.
- At points with vanishing Gaussian curvature, $K = \kappa_1 \kappa_2 = 0$, at least one principal curvature κ_i vanishes and the metric degenerates. In the example of Fig. 2, the triangle mesh is close to a developable surface and thus the isophotes Fig. 2 (middle) are close to straight lines, namely the rulings on the developable surface.

Keeping the first property and eliminating the second one has a simple solution: the purely isophotic metric is regularized with help of the Euclidean metric on Φ . More precisely, we define the *regularized isophotic metric*, henceforth often briefly denoted as ‘isophotic metric’, via the arc length differential

$$ds_i^2 = w \, ds^2 + w^* (ds^*)^2, \quad (3)$$

where ds is the arc element on the surface and ds^* is the arc element on its Gaussian image; $w > 0$ and $w^* \geq 0$ are the weights of the Euclidean and isophotic components, respectively. In the simplest form, the weights will be chosen constant. They can however also be dependent on some appropriate function defined on the surface Φ . The choice of the weights offers a further tool to design appropriate structuring elements for mathematical morphology on Φ .

2.1 Computation on Parametric Surfaces

The computation of the isophotic metric uses only a few basic facts from differential geometry. Let us consider a parameterized surface $\mathbf{x}(u, v)$ and a curve $\mathbf{c}(t)$ on it, given by its preimage $(u(t), v(t))$ in the parameter plane. The first derivative vector $\dot{\mathbf{c}}$ of the curve $\mathbf{c}(t) = \mathbf{x}(u(t), v(t))$ satisfies

$$\dot{\mathbf{c}}^2 = \dot{\mathbf{c}} \cdot \dot{\mathbf{c}} = (\dot{u}\mathbf{x}_u + \dot{v}\mathbf{x}_v)^2 = g_{11}\dot{u}^2 + 2g_{12}\dot{u}\dot{v} + g_{22}\dot{v}^2. \tag{4}$$

Here $\mathbf{x}_u, \mathbf{x}_v$ are the first order partial derivatives of \mathbf{x} ; their inner products,

$$g_{11} = \mathbf{x}_u^2, \quad g_{12} = \mathbf{x}_u \cdot \mathbf{x}_v, \quad g_{22} = \mathbf{x}_v^2, \tag{5}$$

form the symmetric matrix $I = (g_{ik})$ of the *first fundamental form*. It allows us to perform metric computations in the tangent spaces of the surface directly in the parameter domain. For example, the computation of the total arc length of a surface curve by means of its preimage $\mathbf{u} = (u(t), v(t))$ in the parameter domain is done with

$$s = \int_a^b \sqrt{\dot{\mathbf{u}}^t \cdot I \cdot \dot{\mathbf{u}}} dt. \tag{6}$$

The same can be done with the Gaussian image of the surface. Unit normals are computed as

$$\mathbf{n} = \frac{\mathbf{x}_u \times \mathbf{x}_v}{\|\mathbf{x}_u \times \mathbf{x}_v\|} = \frac{\mathbf{x}_u \times \mathbf{x}_v}{\sqrt{g_{11}g_{22} - g_{12}^2}}.$$

Thus, the first derivative of the image curve $\mathbf{c}^*(t) = \gamma(\mathbf{c}(t)) = \mathbf{n}(u(t), v(t))$ on the Gaussian sphere satisfies

$$(\dot{\mathbf{c}}^*)^2 = (\dot{u}\mathbf{n}_u + \dot{v}\mathbf{n}_v)^2 = l_{11}\dot{u}^2 + 2l_{12}\dot{u}\dot{v} + l_{22}\dot{v}^2. \tag{7}$$

Here, the inner products of the partial derivatives of the unit normal field,

$$l_{11} = \mathbf{n}_u^2, \quad l_{12} = \mathbf{n}_u \cdot \mathbf{n}_v, \quad l_{22} = \mathbf{n}_v^2, \tag{8}$$

form the symmetric matrix III of the so-called *third fundamental form*. This matrix, which is not regular at points with vanishing Gaussian curvature K , defines the purely isophotic metric on the surface in exactly the same way as the first fundamental matrix I describes the Euclidean metric on the surface. Finally we see that the regularized isophotic metric has the fundamental matrix

$$M = wI + w^*III = (wg_{ij} + w^*l_{ij}). \tag{9}$$

With help of M , one introduces a Riemannian metric in the parameter domain of the surface, and one can use the familiar framework from differential geometry to perform computations. For example, the total arc length of a curve in the isophotic metric is given by (6) with M instead of I . Figure 3 shows several geodesic curves we have computed on a parametric surface using I and M . Three pairs of input points are each connected with a Euclidean geodesic and a regularized isophotic geodesic. The latter metric forces the geodesic curves to follow the features of the surface.

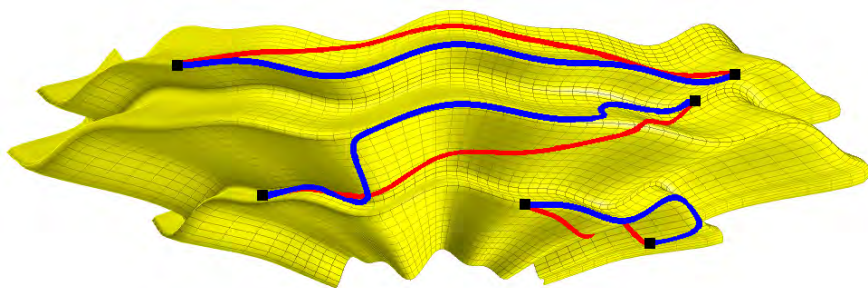


Fig. 3. Geodesic curves on a parametric surface with features: (light colored) computed in the Euclidean metric, i.e. $w = 1$ and $w^* = 0$ in (9); (dark colored) computed in the isophotic metric, for $w = 1$ and $w^* = 2$ in (9).

Remark 1. We may associate with the surface $\mathbf{x}(u, v)$ the 2-dimensional surface $X(u, v) = (\sqrt{w}\mathbf{x}(u, v), \sqrt{w^*}\mathbf{n}(u, v)) \subset \mathbb{R}^6$. Then the canonical Euclidean metric in \mathbb{R}^6 induces on the manifold X exactly the regularized isophotic metric; its first fundamental form agrees with (9). In this sense, the isophotic metric has some relation to work on image manifolds, if we consider the unit normals as a vector valued image on the surface [11].

2.2 Computation on Implicit Surfaces

In view of the increasing importance of implicit representations and the elegance of the level set method for the solution of a variety of problems in geometric computing [1,15,23], it is appropriate to address the computation of the isophotic metric if we are given an implicit representation $F(\mathbf{x}) = 0$ of the surface. There is nothing to do for the Euclidean metric. We simply use the canonical Euclidean metric in \mathbb{R}^3 , described by the identity matrix $E = (\delta_{ij})$. The restriction to any level set surface $\Phi_c : F(\mathbf{x}) = c = const$ is the metric on the surface.

We are now constructing another metric in \mathbb{R}^3 , whose restriction to $F(\mathbf{x}) = 0$ is the desired isophotic metric. For any $\mathbf{x} \in \mathbb{R}^3$ in the domain, where F is defined, the normalized gradient vector $\mathbf{n}(\mathbf{x}) = \nabla F / \|\nabla F\|$, describes the unit normal of the level set of F which passes through \mathbf{x} . Thus, the mapping $\mathbf{x} \mapsto \mathbf{n}(\mathbf{x})$ extends the Gaussian mapping to the set of all level sets of F . The image lies on the unit sphere. The first derivative of this extended Gaussian mapping has the (singular) matrix $J := (\mathbf{n}_x, \mathbf{n}_y, \mathbf{n}_z)$. Hence, the squared (purely) isophotic length $\|\mathbf{v}\|_*^2$ of a vector \mathbf{v} (tangent vector of \mathbb{R}^3 at \mathbf{x}) is

$$\|\mathbf{v}\|_*^2 = (J \cdot \mathbf{v})^2 = \mathbf{v}^t \cdot N \cdot \mathbf{v}, \tag{10}$$

where the matrix $N = (n_{ij}) = J^t \cdot J$ is the Gramian of the partial derivatives of \mathbf{n} . Finally, the matrix

$$\overline{M} = wE + w^*N = (w\delta_{ij} + w^*n_{ij}), \tag{11}$$

describes a Riemannian metric in \mathbb{R}^3 , whose restriction to *any* level set surface $\Phi_c = F^{-1}(c)$ is the corresponding regularized isophotic metric on Φ_c .

Note that the expressions become particularly simple for a *signed distance function* F , since it satisfies $\|\nabla F\| = 1$. Moreover, it is well-known how to efficiently compute the signed distance function to a surface, even if it is given just as a cloud of points [24]. Therefore, the implicit framework can be used to perform computations basically directly on clouds of measurement points.

3 Distance Fields in the Isophotic Metric

A distance function d on a surface Φ is characterized by the Eikonal equation

$$\|\nabla_{\Phi} d\|^2 = 1, \tag{12}$$

where $\nabla_{\Phi} d$ is the surface gradient of d . $\nabla_{\Phi} d$ is a tangential vector of the surface, points in direction of the largest positive directional derivative of d , and its norm is equal to this derivative. For a *parametric representation* $\mathbf{x}(u, v)$ of Φ with first fundamental matrix I , we can express this equation in terms of the ordinary gradient,

$$(\nabla \tilde{d})^t \cdot I^{-1} \cdot \nabla \tilde{d} = 1.$$

Here $\tilde{d} = \tilde{d}(u, v)$ is the representation of the distance function in the parameter domain, so that $\tilde{d}(u, v)$ equals the distance value $d(\mathbf{x}(u, v))$ of the surface point $\mathbf{x}(u, v)$. Moreover, $\nabla \tilde{d} = (\tilde{d}_u, \tilde{d}_v)$ is the ordinary gradient of the bivariate function \tilde{d} . For a distance field in the isophotic metric, we just replace the matrix I by the matrix M from equation (9),

$$(\nabla \tilde{d})^t \cdot M^{-1} \cdot \nabla \tilde{d} = 1. \tag{13}$$

This is a 2D Hamilton-Jacobi equation and therefore the numerical computation of an isophotic distance field to some point set can be done with the fast sweeping algorithm by Tsai et al. [25]. The examples in Fig. 4 have been computed in this way. One can show that the computation of isophotic distance fields on *implicitly defined surfaces* can proceed along the lines of [14]: With \overline{M} from (11) we solve the 3D Hamilton-Jacobi equation,

$$(\nabla d)^t \cdot \overline{M}^{-1} \cdot \nabla d = 1, \tag{14}$$

in a small neighborhood of the surface. Here, a 3D extension [7] of the algorithm by Tsai et al. [25] can be used.

4 Application to Feature Sensitive Morphology on Surfaces

4.1 Continuous Morphology

Let us consider a black image on a white surface. On the surface we have introduced a metric. In our case this is the isophotic metric, but it could be another

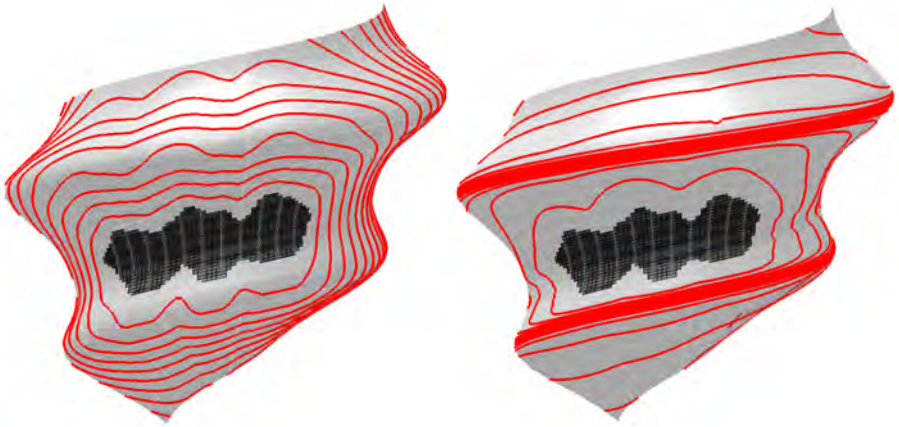


Fig. 4. Level sets to uniformly spaced values of the distance field to a given region in the Euclidean metric (left) and isophotic metric (right). In the isophotic metric, the level sets accumulate at features.

one as well. Then, the distance field to the black part B possesses level sets which are the boundaries of the dilated versions of B . Thus, *dilation* means growth with help of the distance field (see Fig. 4). Likewise, *erosion* can be defined as dilation of the white background, again with the distance field. Combinations of dilation and erosion, which yield *closing* and *opening*, are straightforward. Furthermore, extensions to labelled meshes, in which faces are assigned values from a small set V , is relatively straightforward through the use of series closings on indexed partitions as defined in [8]. For the use of the isophotic metric in *feature sensitive morphology*, we should note the following effects:

- Applying a dilation with high isophotic part ($w^* \gg w$) to a domain adjacent to a feature will make distances across that feature very large and thus avoid a flow across the feature (see Fig. 4, right).
- Application of a dilation with high Euclidean part ($w \gg w^*$) to a domain along a feature will fill interruptions along the feature, but not significantly enlarge the domain across that feature (Fig. 5, left).
- A closing operation of a thin domain along a feature is achieved by applying to it first a dilation with high Euclidean component and then an erosion with high isophotic part (Fig. 5).

4.2 Discrete Morphology

We split the discussion into two parts. At first we discuss local neighborhoods, to be understood as positions of the structuring element. Secondly, we show how to use the neighborhoods – independently from their creation – in the formulation of morphological operators. In both cases we confine ourselves to triangle meshes, but the extension to other cell arrangements, even for manifolds of higher dimension, is rather straightforward.

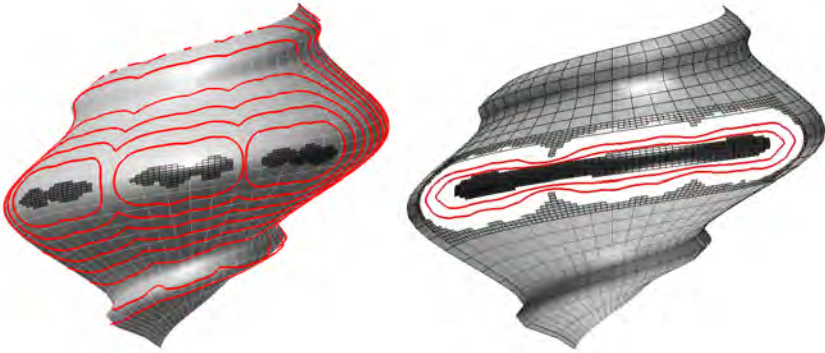


Fig. 5. Continuous morphology: Closing of a domain (black) along a feature: First, a Euclidean dilation (distance field on left side) is applied (result of dilation white on right side), then an erosion with high isophotic part yields the closed domain (black, right).

Neighborhoods. The *combinatorial neighborhood* $N_1(\Delta_i)$ of *depth one* to a triangle Δ_i consists of all triangles in Δ , which share at least one vertex with Δ_i . The neighborhood N_k is defined by iterating the procedure: in step k we add all triangles which share at least a vertex with the boundary of N_{k-1} . For a nearly uniform triangulation, the neighborhoods N_k are good approximants to geodesic circles. For a *neighborhood in the isophotic metric* one has to gather triangles around Δ_i , whose isophotic distance falls below a given threshold. We have implemented the computation of these geodesic discs following an idea by M. Reimers [18], which appears for grids already in [24]. In view of Remark 1 we compute a Euclidean distance field to a triangle on a triangle mesh in \mathbb{R}^6 , which represents a two-dimensional surface. The only difference to the work of [18] is the dimension of ambient space, which is irrelevant for distance computations in the mesh. The examples in Figs. 2, 6, 7 have been computed in this way.

Morphological Operators. Let us first describe the *dilation* of level k of black elements on a white background. At each triangle Δ_i of the triangulation we compute the local neighborhood $N_k(\Delta_i)$ and set the color of Δ_i to black if at least one of the triangles in the neighborhood is black. If the neighborhoods approximate geodesic discs sufficiently well in some metric (e.g. the isophotic metric), we have the following counterpart to the planar case: performing k times a dilation of level one is the same as performing once a dilation of level k . If we use a structuring element (SE) based on the isophotic distance, then it is inevitable that there will be some triangles which lie partly within and partly outside the isophotic distance threshold. A simple solution to this problem would be to assign the triangle to the SE if more than a specified proportion of its surface area is inside the distance boundary. A more flexible approach would be to make use of non-flat SEs [22, p. 441], having values influenced by the proportion of a triangle lying within the distance threshold.



Fig. 6. Discrete morphology: Dilation in the isophotic metric (9) with $w = 0.5$ and $w^* = 0.5$: Starting with the dark triangles (left) we get the result shown (right). Note that the isophotic metric prevents a flow across features.

An *erosion* of level k of black parts is just a dilation of level k applied to the white background. A morphological *closing* operation first applies a dilation of level k , and then an erosion of level k . This fills holes. The *opening* operator applies the erosion before the dilation, which removes thin connections between more compact parts. The width of the bridges to be removed is related to k .

We present examples of discrete morphology on real 3D data. For this purpose we scanned an engineering object (Fig. 6) and a clay model (Fig. 7) with a Minolta VI-900 3D laser scanner, and then triangulated the obtained point clouds to produce the meshes shown in the respective figures. The example in Fig. 6 demonstrates that feature sensitive mathematical morphology can aid the segmentation of an object into its fundamental surfaces; this holds with respect to the definition of local neighborhoods for shape detection, the implementation of region growing algorithms and the processing of the responses from local shape detection filters (images on surfaces). The example in Fig. 7 supports our expectation that morphology in the isophotic metric could be used for artistic effects which are in accordance with the geometry of the surface. Furthermore, the geodesic curves shown in Fig. 3 indicate the usability of the isophotic metric for feature sensitive curve design on surfaces, e.g. for patch layout in connection with high quality freeform surface fitting to clouds of measurement points.

5 Conclusion and Future Research

We have introduced and studied the isophotic metric, discussed some basic computational aspects, and presented examples on its application to feature sensitive morphology on surfaces and geometric design on surfaces. Both the efficient computation as well as the application to morphology require further studies. Promising extensions of the concept are feature sensitive design of energy minimizing splines in the sense of the isophotic metric, and robot path planning, both on surfaces. Another subject of ongoing and future research is a modification of the isophotic metric so that it serves as a tool for image processing in arbitrary dimensions. Here, we interpret a grey value image as a hypersurface, but use – in



Fig. 7. Dilation of the dark triangles (left) on a triangulated surface: (middle) in the Euclidean metric, (right) in the isophotic metric (9) with $w = 0.2$ and $w^* = 0.8$.

accordance with the work of Koenderink and van Doorn [12] – isotropic rather than Euclidean geometry in ambient space.

Acknowledgements. Part of this research has been carried out within the Competence Center *Advanced Computer Vision* and has been funded by the *Kplus* program. This work was also supported by the Austrian Science Fund under grants P14445-MAT and P16002-N05, and by the innovative project “3D Technology” of Vienna University of Technology.

References

1. Bertalmio, M., Méholi, F., Cheng, L.T., Sapiro, G., Osher, S.: Variational problems and partial differential equations on implicit surfaces, CAM Report 02-17, UCLA, April 2002
2. Beucher, S., Blosseville, J. M., Lenoir, F.: Traffic spatial measurements using video image processing. In *Intelligent Robots and Computer Vision, Proc. SPIE*, Vol. 848 (1987) 648–655
3. Caselles, V., Kimmel, R., Sapiro, G., Geodesic active contours, *Intl. J. Computer Vision* **22** (1997), 61–79.
4. Cheng, L.T., Burchard, P., Merriman, B., Osher, S.: Motion of curves constrained on surfaces using a level set approach. UCLA CAM Report 00-36, September 2000
5. Cipolla, R., Giblin, P.: *Visual Motion of Curves and Surfaces*, Cambridge University Press, Cambridge, UK (2000)
6. do Carmo, M.P.: *Differential Geometry of Curves and Surfaces*, Prentice Hall, Englewood Cliffs, NJ (1976)
7. Haider, C., Hönigmann, D.: Efficient computation of distance functions on manifolds by parallelized fast sweeping, *Advanced Computer Vision*, Technical Report 116, Vienna (2003)
8. Hanbury, A.: Mathematical morphology applied to circular data. In P.W. Hawkes, editor, *Advances in Imaging and Electron Physics*, Vol. 128, Academic Press (2003) 123–205
9. Heijmans, H.J.A.M.: *Morphological Image Operators*, Academic Press, Boston (1994)

10. Heijmans, H.J.A.M., Nacken, P., Toet, A., Vincent, L.: Graph Morphology, *Journal of Visual Communication and Image Representation* **3** (1992) 24–38
11. Kimmel, R., Malladi, R., Sochen, N.: Images as embedded maps and minimal surfaces: movies, color, texture and volumetric medical images, *Intl. J. Computer Vision* **39** (2000) 111–129
12. Koenderink, J.J., van Doorn, A.J.: Image processing done right, *ECCV 2002*, LNCS **2350**, Springer-Verlag Heidelberg (2002) 158–172
13. Loménie, N., Gallo, L., Cambou, N., Stamon, G.: Morphological operations on Delaunay triangulations, *Proc. Intl. Conf. on Pattern Recognition*, Vol. 3, Barcelona (2000) 3556–3560
14. Memoli, F., Sapiro, G.: Fast computation of weighted distance functions and geodesics on implicit hyper-surfaces, *J. Comput. Phys.* **173**(2) (2001) 730–764
15. Osher, S., Fedkiw, R.: *Level Set Methods and Dynamic Implicit Surfaces*, Springer-Verlag, New York (2003)
16. Patrikalakis, N. M., Maekawa, T.: *Shape Interrogation for Computer Aided Design and Manufacturing*, Springer-Verlag Berlin Heidelberg New York (2002)
17. J. B. T. M. Roerdink, Mathematical morphology on the sphere, *Proc. SPIE Conf. Visual Communications and Image Processing '90*, Lausanne, pp. 263–271 (1990).
18. Reimers, M.: Computing geodesic distance functions on triangle meshes, Technical Report, Dept. of Informatics, Univ. of Oslo, 2003, (in preparation)
19. Roerdink, J.B.T.M.: Manifold Shape: from Differential Geometry to Mathematical Morphology, in: *Shape in Picture*, Y.L. O et al., eds., Springer-Verlag Berlin Heidelberg New York (1994) 209–223
20. Rössl, C., Kobbelt, L., Seidel, H.-P.: Extraction of feature lines on triangulated surfaces using morphological operators, *Proc. Smart Graphics 2000*, AAAI Spring Symposium, Stanford University.
21. Sapiro, G.: *Geometric Partial Differential Equations and Image Analysis*, Cambridge University Press, Cambridge (2001)
22. Serra, J.: *Image Analysis and Mathematical Morphology*, Academic Press, London (1982)
23. Sethian, J. A.: *Level Set Methods and Fast Marching Methods*, Cambridge University Press, Cambridge (1999)
24. Tsai, Y.-S.R.: Rapid and accurate computation of the distance function using grids, *J. Comput. Phys.* **178**(1) (2002) 175–195
25. Tsai, Y.-S.R., Cheng, L.-T., Osher, S., Zhao, H.-K.: Fast sweeping algorithms for a class of Hamilton-Jacobi equations, *SIAM J. Numerical Analysis* **41**(2) (2003) 673–694
26. Várady, T., Martin, R.: Reverse Engineering, In *Handbook of Computer Aided Geometric Design*, G. Farin, J. Hoschek and M.-S. Kim, eds., Elsevier, (2002) 651–681
27. Verly, J. G., Delanoy, R. L.: Adaptive mathematical morphology for range imagery. *IEEE Transactions on Image Processing* **2**(2) (1993) 272–275
28. Vincent, L.: Graphs and mathematical morphology, *Signal Processing* **16** (1989) 365–388